Scientia Iranica, Vol. 9, No. 2, pp 157–161
© Sharif University of Technology, April 2002

SCIENTIA
IRANICA

Research Note

Crystallization Behavior of Ni-Nb Amorphous Alloys

M.H. Enayati[1]

The crystallization behavior of Ni-Nb amorphous alloys containing 20, 40 and 60 at.% Nb was studied with a combination of differential scanning calorimetry and x-ray diffractometry. The crystallization sequences were analyzed with regard to the free energy versus composition curves of Ni-Nb system. The crystallization of $Ni_{80}Nb_{20}$ and $Ni_{40}Nb_{60}$ amorphous alloys appeared to occur with a primary crystallization mechanism. Whereas $Ni_{60}Nb_{40}$ amorphous alloy crystallized with an eutectic crystallization behavior. The $Ni_{60}Nb_{40}$ amorphous alloy was found to be the most stable alloy on heating among three investigated Ni-Nb amorphous alloys.

INTRODUCTION

Amorphous alloys have unique and useful properties which are not found when the alloy is in the crystalline state. To some extent, the properties of amorphous materials are influenced mainly by their short-range order. Amorphous metallic alloys exhibit high strength and toughness, low magnetic losses, high corrosion resistance, low degradation of mechanical properties in irradiation environments and improved catalytic properties [1,2]. This combination of physical and mechanical properties in amorphous metallic alloys has led to commercial applications especially in the field of magnetic materials. Since the amorphous structure always has a higher free energy than a combination of crystalline phases, it is susceptible to crystallization. The crystallization of amorphous alloys has a number of practical implications. The loss of many desirable properties on crystallization imposes a strict limit on the operating times at elevated temperatures. Additionally, the partial or full crystallization of amorphous alloys may lead to novel and useful microstructures, unobtainable by other routes.

The Ni-Nb amorphous alloys have been successfully produced by several techniques such as splat quenching [3], vapour quenching [4] and mechanical alloying [5,6]. However, the crystallization behavior of Ni-Nb amorphous alloys has not been investigated in detail. Koch et al. [5] studied the crystallization of $Ni_{60}Nb_{40}$ amorphous alloy prepared by melt spinning and mechanical alloying. They found that the crystallization of $Ni_{60}Nb_{40}$ amorphous alloy occurs in two stages. Although the crystallization structure in the first stage was not identified, the final crystallization products, after the second stage for both melt spun and mechanically alloyed samples, consisted of Ni_3Nb and Ni_6Nb_7 phases. Khlyntsev et al. [7] found that the crystallization of $Ni_{70}Nb_{30}$ amorphous alloy produced by rapid solidification also includes two stages. The first stage involves the formation of solid solution crystals of 30-40° A in size. The x-ray diffraction traces taken at this stage showed no difference from the amorphous state. This structure decomposed to a mixture of two equilibrium phases, Ni_3Nb and Ni_6Nb_7 in the second stage of crystallization. Ruhl et al. [3] also found the Ni_6Nb_7 and Ni_3Nb phases present after full crystallization of splat quenched $Ni_{59}Nb_{41}$ amorphous alloy, although they also observed a complex transition at the beginning of crystallization.

The aim of the present work was to study the thermal stability and crystallization sequence of some Ni-Nb amorphous alloys prepared by mechanical alloying and melt spinning.

EXPERIMENTAL PROCEDURES

Ni-Nb amorphous alloys containing 20, 40 and 60 at.% Nb were produced by Mechanical Alloying (MA) and Melt Spinning (MS). To prevent oxidation or nitridation of materials, mechanical alloying and melt spinning were performed under an Ar atmosphere. The details of mechanical alloying and melt spinning procedures are given elsewhere [8]. The crystallization

1. *Department of Materials Engineering, Isfahan University of Technology, Isfahan 84154, I.R. Iran.*

behavior of amorphous samples was studied using Differential Scanning Calorimetry (DSC) in a TA2200 thermal analyser fitted with a 2010 DSC module using a constant heating rate of 10 K/min from 150 to 670°C under a dynamic Ar atmosphere. An oxygen trap was used to avoid any possible O_2 contamination in the Ar flow. After each DSC scan a subsequent second scan was performed, without disturbing the sample, to obtain a base-line. The onset temperatures of the DSC peaks were taken as the temperature at which the DSC signal deviated from the base-line by about 1% of the maximum peak value. The temperature at which the DSC peak reached its maximum value was taken as the peak temperature.

To determine what structural transitions occurred during crystallization, samples were heated in the DSC under identical conditions but were cooled after each DSC peak and analyzed by X-Ray Diffractometry (XRD) in a Philips PW1729 diffractometer using filtered CuKα radiation ($\lambda = 0.1542$ nm).

Those compositions with an end temperature of crystallization higher than or close to 670°C, which corresponds to the limit of the TA2010 DSC used here, were annealed in a furnace at 760°C for 1.5 h to ensure full crystallization. Annealing was performed inside glass tubes using a conventional tube furnace. The glass tubes were evacuated to a pressure lower than 1×10^{-5} mbar and then sealed.

The composition of samples was determined using a Cameca Su30 electron microprobe analyzer with a wavelength-dispersive x-ray spectrometer (WDX) attachment.

RESULTS

$Ni_{80}Nb_{20}$, $Ni_{60}Nb_{40}$ and $Ni_{40}Nb_{60}$ alloys were successfully amorphized by mechanical alloying. The amorphous powders had a nearly spherical shape and nearly uniform particle size of 60 μm. By melt spinning, however, it was possible to produce amorphous structures only for $Ni_{60}Nb_{40}$ composition. Melt spinning of $Ni_{60}Nb_{40}$ alloy resulted in continuous ribbons with typical dimensions of 20-25 μm in thickness and 1.5 mm in width. Figure 1 shows XRD traces from $Ni_{80}Nb_{20}$, $Ni_{60}Nb_{40}$ and $Ni_{40}Nb_{60}$ amorphous alloys.

As shown in this figure, all samples exhibited a diffuse halo, characteristic of a fully amorphous structure, without any indication of additional crystalline phases. It is interesting to note that in spite of basic differences in the amorphization mechanism by mechanical alloying and melt spinning, the structure of MA and MS $Ni_{60}Nb_{40}$ amorphous alloys, as seen by XRD, are quite similar.

The compositions of $Ni_{80}Nb_{20}$, $Ni_{60}Nb_{40}$ and $Ni_{40}Nb_{60}$ amorphous alloys are shown in Table 1. For MS $Ni_{60}Nb_{40}$ sample the nominal and measured

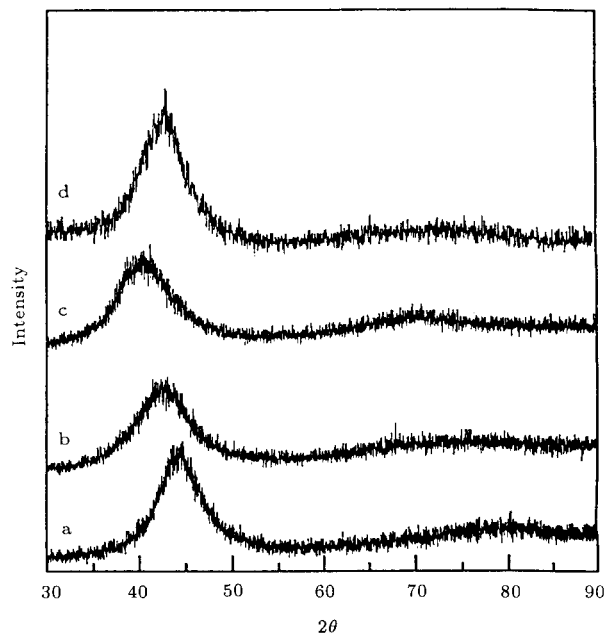

Figure 1. XRD traces from a) MA $Ni_{80}Nb_{20}$, b) MA $Ni_{60}Nb_{40}$, c) MA $Ni_{40}Nb_{60}$ and d) MS $Ni_{60}Nb_{40}$ amorphous alloys.

Table 1. Composition of MA and MS amorphous alloys.

Sample	Measured Composition (at.%)				
	Ni	Nb	Fe	Cr	Si
MA $Ni_{80}Nb_{20}$	77.78	19.40	2.58	0.24	-
MA $Ni_{60}Nb_{40}$	58.30	38.81	2.62	0.27	-
MA $Ni_{40}Nb_{60}$	38.40	58.09	3.14	0.35	-
MS $Ni_{60}Nb_{40}$	60.10	39.85	-	-	0.05

compositions were close to each other indicating minimal loss of elements during melt spinning. A small amount of Si impurity was picked up from the SiO_2 quartz nozzle during melt spinning. MA samples were contaminated by Fe and Cr due to wear of the milling media.

The crystallization behavior of Ni-Nb amorphous alloys was studied with a combination of DSC and XRD. Figure 2 shows the DSC traces from $Ni_{80}Nb_{20}$, $Ni_{60}Nb_{40}$ and $Ni_{40}Nb_{60}$ amorphous alloys prepared by mechanical alloying. The DSC traces from melt spun $Ni_{60}Nb_{40}$ amorphous ribbons are also included for comparison reasons.

As seen in this figure, the $Ni_{80}Nb_{20}$ amorphous alloy exhibited two crystallization exotherms and the $Ni_{60}Nb_{40}$ and the $Ni_{40}Nb_{60}$ amorphous alloys showed a single crystallization exotherm on the DSC traces over the temperature range studied. The onset and peak crystallization temperatures, T_o and T_p, for each of the three amorphous alloys are listed in Table 2. Crystallization products after the first crystallization exotherm and also after further annealing at 760°C for

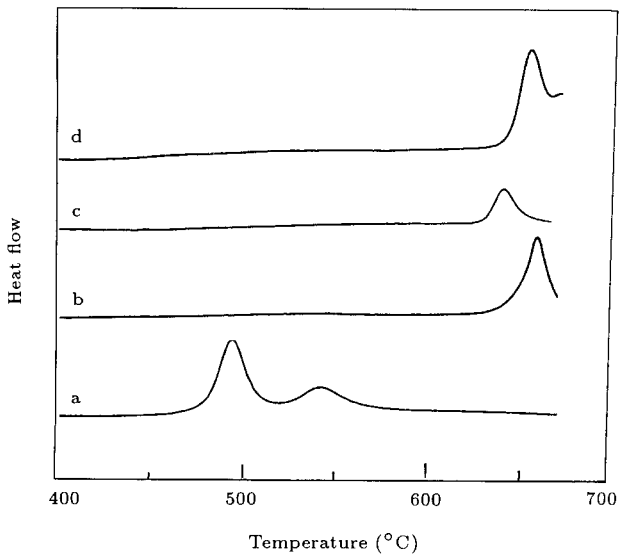

Figure 2. DSC traces from a) MA $Ni_{80}Nb_{20}$, b) MA $Ni_{60}Nb_{40}$, c) MA $Ni_{40}Nb_{60}$ and d) MS $Ni_{60}Nb_{40}$ amorphous alloys.

Table 2. Onset and peak crystallization temperatures (T_o and T_P°C) for MA and MS amorphous alloys (errors $\leq$ 1.5°C).

Composition	T_o	T_{P1}	T_{P2}
MA $Ni_{80}Nb_{20}$	462	494	545
MA $Ni_{60}Nb_{40}$	629	662	-
MA $Ni_{40}Nb_{60}$	630	643	-
MS $Ni_{60}Nb_{40}$	632	658	-

1.5 h were identified using XRD although several XRD peaks remained unknown.

For MA $Ni_{80}Nb_{20}$ amorphous alloy, the XRD traces taken after continuous heating in the DSC up to 515°C (through the first DSC exotherm in Figure 2a) exhibited several crystalline peaks together with an amorphous halo. The presence of the halo indicated that the crystallization process was incomplete after the first DSC exotherm. The low intensity and spread of crystalline peaks did not allow identification of the crystallization product at this stage. Continuous heating through the second DSC exotherm led to a fully crystallized structure containing the equilibrium Ni_8Nb and Ni_3Nb phases and an unknown phase.

For MA $Ni_{60}Nb_{40}$ amorphous alloy, the XRD traces taken after continuous heating in the DSC up to 670°C showed a fully crystallized structure containing the broadened diffraction peaks of Ni_3Nb and Ni_6Nb_7 along with some unknown peaks. After isothermal annealing in a furnace at 760°C for 1.5 h the XRD traces again included mostly the sharp Ni_3Nb and Ni_6Nb_7 peaks, although some of the unknown peaks vanished and instead several further unknown peaks appeared on the XRD traces. It is worth noting that the crystallization temperatures, as shown in Table 2, as well as the crystallization products for MS $Ni_{60}Nb_{40}$ amorphous alloy were similar to those for MA $Ni_{60}Nb_{40}$ amorphous alloy.

For MA $Ni_{40}Nb_{60}$ amorphous alloy, the XRD traces taken after continuous heating in the DSC up to 670°C showed a partially crystallized structure consisting of the diffraction peaks of Ni_6Nb_7 phase and some unknown peaks along with an amorphous halo. After isothermal annealing in a furnace at 760°C for 1.5 h the amorphous halo disappeared and the Ni_6Nb_7 peaks became stronger. In addition, several further unknown peaks appeared on the XRD traces.

The XRD traces after isothermal annealing at 760°C for 1.5 h for $Ni_{80}Nb_{20}$, $Ni_{60}Nb_{40}$ and $Ni_{40}Nb_{60}$ alloys included the same unknown peaks which had much higher intensity for alloys with higher Nb content. The unknown phase could not be indexed to any known oxide or nitride of Ni or Nb. The unknown peaks appeared not to be related to Fe and Cr impurities, as the same unknown peaks were observed for MS $Ni_{60}Nb_{40}$ sample which excludes these impurities.

Disregarding the unknown phases, the final crystallization structure of $Ni_{80}Nb_{20}$ and $Ni_{60}Nb_{40}$ amorphous alloys was consistent with the expected equilibrium structure from the Ni-Nb phase diagram. The fully crystallized structure of $Ni_{40}Nb_{60}$ amorphous alloy did not contain the Nb phase which did not agree with the phase diagram.

DISCUSSION

Crystallization Sequence

The crystallization sequence of Ni-Nb amorphous alloys can be analyzed by means of free energy versus composition curves for different phases as shown in Figure 3. According to Figure 3, for each of three amorphous alloys, $Ni_{80}Nb_{20}$, $Ni_{60}Nb_{40}$ and $Ni_{40}Nb_{60}$, there are several possible paths with which amorphous-to-crystalline transformation can occur. These paths are summarized in Table 3.

Disregarding the unknown phases, the crystallization sequences for three Ni-Nb amorphous alloys were found to be as follows:

$$\text{MA } Ni_{80}Nb_{20} \xrightarrow{462^\circ C} \text{partially crystallized} \longrightarrow Ni_8Nb + Ni_3Nb,$$

$$\text{MS \& MA } Ni_{60}Nb_{40} \xrightarrow{629^\circ C} Ni_3Nb + Ni_6Nb_7,$$

$$\text{MA } Ni_{40}Nb_{60} \xrightarrow{630^\circ C} Ni_6Nb_7 + \text{amorphous phase} \longrightarrow Ni_6Nb_7.$$

The MA $Ni_{80}Nb_{20}$ amorphous alloy crystallizes in two stages with an onset temperature of T_o = 462°C

Table 3. Possible paths for crystallization of $Ni_{80}Nb_{20}$, $Ni_{60}Nb_{40}$ and $Ni_{40}Nb_{60}$ amorphous alloys ("a" refers to amorphous phase).

Composition	Possible Crystallization Sequences
a-$Ni_{80}Nb_{20}$	(1) Ni+a_1 .....primary crystallization
	(2) Ni_8Nb+a_2 .....primary crystallization
	(3) Ni_3Nb .....polymorphic crystallization
	(4) Ni_8Nb+Ni_3Nb .....eutectic crystallization
	(5) Ni_8Nb+Ni_6Nb_7 .....eutectic crystallization
	(6) Ni+Ni_3Nb .....eutectic crystallization
a-$Ni_{60}Nb_{40}$	(1) Ni_3Nb+a_3 .....primary crystallization
	(2) Ni_6Nb_7+a_4 .....primary crystallization
	(3) Ni_6Nb_7+Ni_3Nb .....eutectic crystallization
	(4) Ni_6Nb_7+Ni_8Nb .....eutectic crystallization
a-$Ni_{40}Nb_{60}$	(1) Nb+a_5 .....primary crystallization
	(2) Ni_6Nb_7 .....polymorphic crystallization
	(3) Nb+Ni_6Nb_7 .....eutectic crystallization

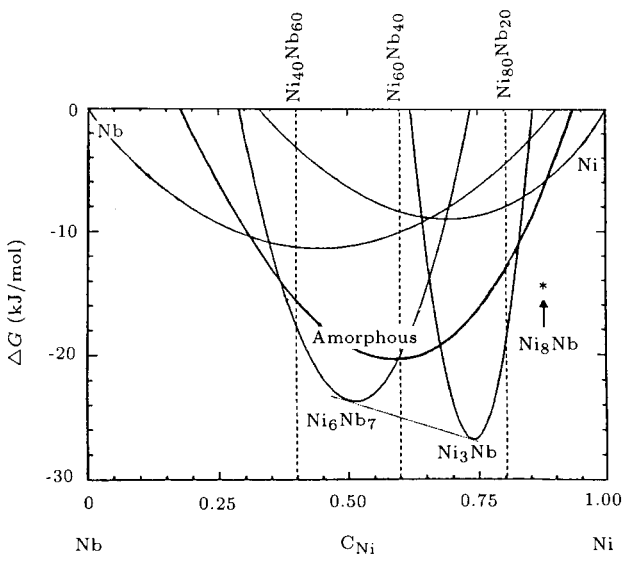

Figure 3. Free energy versus composition diagram for Ni-Nb system at 350°C (after Bormann and Busch [9]).

and peak temperatures of 494 and 545°C. The crystallization products after the first DSC exotherm could not be identified, making it impossible to characterize the amorphous-to-crystalline transition during the first crystallization exotherm for this alloy. Nevertheless, the presence of an amorphous halo on corresponding XRD traces, taken after the first crystallization exotherm, suggests that the crystallization of this alloy occurs with a primary crystallization mechanism. As shown in Table 3, there are two possible primary crystallization reactions for the $Ni_{80}Nb_{20}$ amorphous alloy, paths 1 and 2, which incorporate Ni and Ni_8Nb phases respectively. The structure after second crystallization exotherm, however, consists of Ni_8Nb and Ni_3Nb phases without any traces of Ni, suggesting that the amorphous $Ni_{80}Nb_{20}$ alloy crystallizes with the primary crystallization reaction via path 2 rather than path 1.

The crystallization of amorphous $Ni_{60}Nb_{40}$ alloy prepared by MA starts at T_o = 629°C with peak temperature of 662°C. The crystallization products, after continuous heating in DSC up to 670°C, consisted of a mixture of Ni_3Nb and Ni_6Nb_7 phases without any indication of an amorphous phase remaining from a primary crystallization stage. Further annealing at 760°C led to the formation of a further unknown phase. Nevertheless, the main crystallization products remained unchanged. These results suggest that the $Ni_{60}Nb_{40}$ amorphous alloy crystallizes with an eutectic crystallization behavior, i.e., simultaneous formation of two crystalline phases, Ni_3Nb and Ni_6Nb_7 in one stage (path 3 in Table 3). XRD analysis showed that the sequential crystallization behavior of the MS $Ni_{60}Nb_{40}$ amorphous alloy is similar to that for MA $Ni_{60}Nb_{40}$ amorphous alloy.

The MA $Ni_{40}Nb_{60}$ amorphous alloy crystallizes at T_o = 630°C with a peak temperature of 643°C. The crystallization appeared to occur with a primary crystallization mechanism (path 1 in Table 3). XRD traces, taken after continuous heating in the DSC up to 670°C, include an amorphous halo remaining from an incomplete crystallization together with Ni_6Nb_7 peaks and several unknown peaks. After further annealing at 760°C a fully crystallized structure consisting mainly of Ni_6Nb_7 was obtained without any indication of Nb. The formation of the Ni_6Nb_7 compound as a product of the primary crystallization is, however, not predicted from Figure 3. This phase may arise from a subsequent second crystallization exotherm, at temperatures higher than 670°C, which overlaps with the first crystallization exotherm. During this second stage of crystallization the remaining amorphous matrix transforms to Nb and Ni_6Nb_7 phases.

The lack of Nb in the structure after the first and second stages of crystallization is also not in agreement with Figure 3. As pointed out in the previous section the fully crystallized structure of all three investigated Ni-Nb alloys contained same unknown phases which were more pronounced for higher Nb content compositions, indicating that Nb is the main participant in these unknown phases. The lack of Nb in the crystallization products of $Ni_{40}Nb_{60}$ is likely related to the formation of these unknown phases.

Thermal Stability

Table 2 shows the onset and peak crystallization temperatures (T_o and T_P) of $Ni_{80}Nb_{20}$, $Ni_{60}Nb_{40}$ and $Ni_{40}Nb_{60}$ amorphous alloys. As seen the eutectic composition $Ni_{60}Nb_{40}$ has the highest peak crystallization temperature among the three alloys. The onset temperature of crystallization (T_o) can be taken as a criterion to compare the relative thermal stability of these three amorphous alloys. $Ni_{80}Nb_{20}$ has the lowest thermal stability against crystallization. Increasing Nb content from 20 to 40 at.% increases thermal stability significantly. However, further increase in Nb content to 60 at.% appears to have little effect on thermal stability, although the peak crystallization temperature T_P decreases. This is in contrast to the results given by Barbee et al. [4] for Ni-Nb amorphous alloys prepared by vapour quenching. Thermal stability was determined by the first appearance of crystalline phases at high temperatures using in-situ XRD with temperature intervals of 20°C. The crystallization temperature was found to be significantly higher around the eutectic composition, $Ni_{60}Nb_{40}$. Obviously this method does not give accurate data as the temperature intervals of 20°C are not small enough to determine the onset of crystallization. Petzoldt [6] measured the peak crystallization temperature for a series of MA Ni-Nb amorphous alloys in the composition range of 20-80 at.% Ni. The peak crystallization temperature, T_P, was found to be a steep function of composition. In the range between 20-60 at.% Ni it was nearly constant around 670°C (at heating rate 40 K/min). The crystallization temperature dropped by 100°C in composition range of 70-80 at.% Ni The behavior of T_P reported by Petzoldt is similar but not exactly the same as the present study, which shows a slight T_P decrease as the Ni concentration increases from 40 to 60 at.%.

CONCLUSIONS

The crystallization behavior of $Ni_{80}Nb_{20}$, $Ni_{60}Nb_{40}$ and $Ni_{40}Nb_{60}$ amorphous alloys prepared by mechanical alloying and melt spinning was studied with a combination of DSC and XRD. The results showed that the crystallization of $Ni_{80}Nb_{20}$ and $Ni_{40}Nb_{60}$ amorphous alloys occurs with a primary crystallization mechanism. Whereas $Ni_{60}Nb_{40}$ amorphous alloy crystallized with an eutectic crystallization behavior. The sequential crystallization behavior of the mechanically alloyed and melt spun amorphous alloys was found to be very similar. The eutectic composition $Ni_{60}Nb_{40}$ had the highest stability against crystallization among the three Ni-Nb amorphous alloys.

ACKNOWLEDGMENTS

The author would like to thank Prof. B. Cantor and Dr. P. Schumacher at the Department of Materials, University of Oxford for their fruitful discussions and invaluable suggestions.

REFERENCES

1. Polk, D.E. and Giessen, B.C. "Metallic Glasses", Gilman, J.J. and Leamy, H.J., Eds., *Metals Park, ASM*, Ohio, p 27 (1978).
2. Luborsky, F.E., *Encyclopedia of Materials Science and Engineering*, Bever, M.B., Ed., Pergamon Press, Oxford, **4**, p 2963 (1986).
3. Ruhl, R.C., Giessen, B.C., Cohen, M. and Grant, N.J., *Acta Metall.*, **15**, p 1693 (1967).
4. Barbee, T.W., Holmes, W.H., Keith, D.L. and Pyzyna, M.K., *Thin Solid Films*, **45**, p 591 (1977).
5. Koch, C.C., Cavin, O.B., McKamey, C.G. and Scarbrough, J.O., *Appl. Phys. Lett.*, **43**, p 1017 (1983).
6. Petzoldt, F., *J. Less-Com. Met*, **140**, p 85 (1988).
7. Khlyntsev, V.P., Potapov, L.P. and Kiriyenko, V.I., *Phys. Met. Metall.*, **47**, p 176 (1980).
8. Enayati, M.H., Chang, I.T.H., Schumacher, P. and Cantor, B., *Materials Science Forum*, **235**, p 85 (1997).
9. Bormann, R. and Busch, R. "New Materials by Mechanical Alloying Technology", Arzt, E. and Schultz, L., Eds., *DGM, Oberursel*, p 73 (1989).